

SUPPORTING INFORMATION

Supporting Information

H₂O₂ Accumulation Promoting Internalization of ox-LDL in Early Atherosclerosis Revealed via a Synergistic Dual-Functional NIR Fluorescence Probe

Hui Wang,^{*†[a]} Jingjing Guo,^{†[a]} Tiancong Xiu,^[a] Yue Tang,^{*[d]} Ping Li,^{*[a,c]} Wei Zhang,^[a]
Wen Zhang,^[a] Bo Tang^{*[a,b]}

Table of Contents

Experimental Procedures	3
1. Materials and instruments	3
2. Synthesis of HV-AS	3
3. Detection of absorbance and fluorescence spectra of the HV-AS.....	3
4. The Förster-Hoffmann equation	3
5. Kinetic parameters of HV-AS towards H ₂ O ₂ and viscosity.....	3
6. Stability of HV-AS in different solution	3
7. Selectivity of HV-AS for H ₂ O ₂ and viscosity.....	3
8. Anti-interference ability for H ₂ O ₂ detection.....	4
9. Fluorescence quantum yield of HV-AS	4
10. Photostability test.....	4
11. Co-localization experiment of HV-AS	4
12. Detection of ectogenic and endogenous H ₂ O ₂ and viscosity in cells.....	4
13. Fluorescence imaging of HV-AS in cells.....	4
14. Immunofluorescence staining.....	4
15. <i>In vivo</i> toxicity of HV-AS	4
16. Establishment of mice model	4
17. Fluorescence imaging of HV-AS in mice.....	5
18. Hemolysis test.....	5
Results and Discussion	5
References	20
Author Contributions	20

Experimental Procedures

1. Materials and instruments

2,3,3-trimethylindolenine, iodoethane, 4-bromomethylphenylboronic acid pinacol ester, KI, malonitrile, 4-hydroxyisophthalaldehyde, indocyanine green (ICG), nystatin, lipopolysaccharide (LPS), N-acetylcysteine (NAC) were purchased from Shanghai Aladdin Biochemical Technology Co., Ltd. and Shanghai Macklin Biochemical Co., Ltd. Ethyl acetate (EA), acetonitrile (MeCN), petroleum ether, ethanol (EtOH), pyridine, dichloromethane (DCM), toluene, tetrahydrofuran (THF), acetone, methanol (MeOH), dimethyl sulfoxide (DMSO) and glycerol were bought from Sinopharm Chemical Reagent Co., Ltd. Solvents were used without further purification. Paraformaldehyde (POM), LD-Tracker Green, ER-Tracker Green, Mito-Tracker Green, Lyso-Tracker Green and Hoechst 33342 were all bought from Beyotime.

Primary antibodies and inhibitors were using for biological experiments, included Recombinant Anti-cd40 Rabbit Monoclonal Antibody (1:200, Abcam, ab188181, UK), IL-1 β Rabbit Polyclonal Antibody (1:200, Proteintech, 26048-1-AP, China), LOX-1 Rabbit Polyclonal Antibody (1:200, Proteintech, 11837-1-AP, China), Goat Anti-Rabbit IgG H&L (1:1000, Abcam, ab175471, UK), setanaxib (NOX 1/4 inhibitor, aladdin, 1218942-37-0, China), apocynin (NOX inhibitor, MCE, 498-02-2, China).

The main instruments used during the experiments include the four-stage rod time-of-flight mass spectrometer (Bruker Maxis), the nuclear magnetic resonance spectrometer (Bruker), the UV-Vis spectrophotometer (Thermo Fisher Scientific), the fluorescence spectrometer (Hitachi F-7000 fluorescence spectrophotometer, HITACHI), the enzyme standard (Rayto), the SP8 laser confocal microscope (Leica), IVIS[®] Lumina III *in vivo* imaging system (PerkinElmerzei), the high-speed centrifuge (Eppendorf), NDJ-8S rotational viscometer, etc.

2. Synthesis of HV-AS

Synthesis of compound 1^[1]: 2,3,3-trimethylindolenine (25 mmol, 4.01 mL) and iodoethane (27 mmol, 2.01 mL) were dissolved in MeCN (10 mL), the reaction was heated up to 80°C (reflux) under stirring for 24 h. The crude product was precipitated in ethyl acetate (EA) three times to acquired Pink solids. **Compound 1** was obtained (4.47 g, yield 95%).

Synthesis of compound 2^[2]: 4-bromomethylphenylboronic acid pinacol ester (6 mmol, 1.782 g) and Cs₂CO₃ (6 mmol, 1.955 g) were dissolved in MeCN (20 mL) for 10 min. And then, 4-hydroxyisophthalaldehyde (3 mmol, 0.450 g) and KI (3 mmol, 0.498 g) were added. The reaction was proceeded for 12 h at 60°C in dark environment. After accomplishment, the mixtures were purified though column chromatography (EA: petroleum ether = 1:2, v/v) to get **compound 2** (0.85 g, yield 78%).

Synthesis of HV-AS: Compound 1 (0.5 mmol, 0.047 g) and **Compound 2** (0.5 mmol, 0.092 g) were dissolved in ethanol and were refluxed for 6h at 80°C in nitrogen atmosphere. After 6 h, malonitrile (0.9 mmol, 0.060 g) and pyridine (120 μ L) were added to the reaction, and the reaction continued for 6h under the same conditions. The reaction was stopped and purified by thin layer chromatography. Solutions were EA: DCM: petroleum ether = 1:1:3 (v/v/v) that it can obtain **HV-AS** (0.086 g, yield 30%). ¹H NMR (400 MHz, CDCl₃) δ 8.13 (s, 1H), 7.92 (d, *J* = 8.0 Hz, 2H), 7.67 (s, 1H), 7.47 (d, *J* = 8.0 Hz, 2H), 7.13 (d, *J* = 8.7 Hz, 2H), 7.05 (d, *J* = 7.4 Hz, 1H), 6.80 (t, *J* = 7.3 Hz, 1H), 6.56 (d, *J* = 7.8 Hz, 1H), 5.34 (s, 2H), 5.11 (d, *J* = 11.32 Hz, 1H), 4.74 (d, *J* = 11.3 Hz, 1H), 4.27 (d, *J* = 5.3 Hz, 1H), 3.71–3.66 (m, 2H), 1.38 (s, 12H), 1.36 (s, 6H), 1.27 (t, *J* = 7.32 Hz, 3H). ¹³C NMR (101 MHz, CDCl₃) δ 159.56, 158.44, 157.58, 144.62, 137.72, 137.54, 135.64, 133.56, 132.36, 129.98, 128.02, 126.66, 124.80, 121.48, 119.21, 114.11, 113.13, 112.26, 111.77, 105.58, 84.18, 71.34, 37.48, 36.82, 30.27, 28.35, 27.89, 24.98. HRMS (ESI) *m/z* calculated for C₃₇H₃₉BN₃O₃⁺[M]⁺ 584.3079, found 584.3098.

3. Detection of absorbance and fluorescence spectra of the HV-AS.

The **HV-AS** was dissolved in MeCN to obtain a 10 mM **HV-AS** solution, which was diluted with PBS (30% MeCN) and MeOH-glycerol solutions to the necessary concentration in a quartz colorimetric dish. Absorbance spectra of **HV-AS** was collected from 450 nm to 650 nm in the H₂O₂ channel and from 310 nm to 500 nm in the viscosity channel.

All fluorescence measurements were obtained with Hitachi F-7000 fluorescence spectrophotometer at room temperature. The fluorescence of H₂O₂ channel was collected between 590 nm and 800 nm under the excitation of 570 nm. The fluorescence of viscosity channel was acquired between 400 nm and 700 nm under the excitation of 360 nm.

4. The Förster-Hoffmann equation

According to Förster-Hoffmann equation,^[3] the relationship between fluorescence intensity of **HV-AS** and viscosity can be calculated.

$$\log F = k \log \eta + C$$

In this equation, η *k* is solution viscosity, *F* is fluorescence emission intensity in different solution, *k* is **HV-AS** related constants, *c* is constants of temperature and concentration.

5. Kinetic parameters of HV-AS towards H₂O₂ and viscosity

H₂O₂ channel: the fluorescence of 20 μ M **HV-AS** at 680 nm was measured after adding 0 μ M and 500 μ M H₂O₂, with measurements taken every 2 min for a total of 30 min. When the excitation wavelength is 570 nm, fluorescence intensity was measured at 680 nm. Viscosity channel: In different MeOH-glycerol systems (v/v = 10:0 and 2:8), the fluorescence of 20 μ M **HV-AS** was measured every 2 seconds over a period of 30 minutes. Then, kinetic parameter was calculated.

6. Stability of HV-AS in different solution

HV-AS (20 μ M) was dissolved in solutions of different polarities, including toluene, tetrahydrofuran (THF), ethyl acetate (EA), ethanol (EtOH), acetone, methanol (MeOH), acetonitrile (MeCN), dimethyl sulfoxide (DMSO), water (H₂O), glycerol, and a mixture of methanol and glycerol in a 2:8 (v/v) ratio. The solutions were then incubated at 37°C for 30 minutes. The excitation wavelength for H₂O₂ imaging was set to 561 nm, with a light collection window range of 570–720 nm. The excitation wavelength for viscosity imaging was set to 405 nm, with a light collection window range of 420–550 nm.

7. Selectivity of HV-AS for H₂O₂ and viscosity

In this experiment, the analytes include 200 μ M H₂O₂, 10 μ M reactive oxygen species (¹O₂, ClO⁻, O₂⁻, \cdot OH, TBHP, ONOO⁻, NO),

SUPPORTING INFORMATION

200 μM metal ions (Na^+ , K^+ , Fe^{2+} , Zn^{2+} , Mg^{2+} , Ca^{2+}), 200 μM anions (NO_2^- , NO_3^- , $\text{S}_2\text{O}_3^{2-}$, $\text{C}_5\text{H}_7\text{O}_5\text{COO}^-$, HS^- , HSO_3^-), 200 μM reactive sulfur species (GSH, Hcy, Cys) and glycerol. These analytes were incubated with **HV-AS** in buffer with 30% MeCN, and then the fluorescence intensity of **HV-AS** was measured at 680 nm under 570 nm excitation. Meanwhile, the analytes were incubated with **HV-AS** in methanol, and then the fluorescence intensity of **HV-AS** (20 μM) was measured at 537 nm under 360 nm excitation.

8. Anti-interference ability for H_2O_2 detection

The analytes include 10 μM reactive oxygen species ($^1\text{O}_2$, ClO^- , $\text{O}_2^{\cdot-}$, $\cdot\text{OH}$, TBHP, ONOO^- , NO), 200 μM metal ions (Na^+ , K^+ , Fe^{2+} , Zn^{2+} , Mg^{2+} , Ca^{2+}), 200 μM anions (NO_2^- , NO_3^- , $\text{S}_2\text{O}_3^{2-}$, $\text{C}_5\text{H}_7\text{O}_5\text{COO}^-$, HS^- , HSO_3^-), 200 μM reactive sulfur species (GSH, Hcy, Cys). These analytes were co-incubated with 20 μM **HV-AS** and 200 μM H_2O_2 in buffer with 30% MeCN, respectively. And then, the fluorescence intensity of **HV-AS** was measured at 680 nm under 570 nm excitation. The fluorescence intensity of 20 μM **HV-AS** and 0 μM H_2O_2 group was defined as 1. The control group was 20 μM **HV-AS** + 200 μM H_2O_2 group.

9. Fluorescence quantum yield of HV-AS

The fluorescence yield of **HV-AS** in different solvents with or without H_2O_2 were calculated according to previous report,^[3,4] Indocyanine green (ICG) was used as the reference ($\Phi_f = 0.13$ in DMSO) to calculate the fluorescence quantum yield of **HV-AS** at 680 nm. Quinine sulfate ($\Phi_f = 0.54$ in 0.1M H_2SO_4) was used as the reference to calculate the fluorescence quantum yield of **HV-AS** at 537 nm.

10. Photostability test

The fluorescence of **HV-AS** at 680 nm was measured after treatment with 0 μM and 500 μM H_2O_2 for 20 min at 37°C. Fluorescence was measured every 2 seconds over a period of 30 minutes upon continuous laser irradiation at 570 nm for 1800s.

RAW 264.7 cells were incubated with 20 μM **HV-AS** for 30 min at 37°C, the cells were continuously irradiated with a laser ($\lambda_{\text{ex}} = 561$ nm) at least 30 min. The fluorescence was collected every 3 minutes over a period of 33 minutes in H_2O_2 channel (570–720 nm) under excitation at 561 nm and in viscosity channel (420–550 nm) under excitation at 405 nm.

11. Co-localization experiment of HV-AS

The fluorescence of **HV-AS** (20 μM) was collected at 570–720 nm under excitation at 561 nm. LD-Tracker Green (0.5 μM , $\lambda_{\text{ex}} = 488$ nm, $\lambda_{\text{em}} = 490$ –560 nm), ER-Tracker Green (0.5 μM , $\lambda_{\text{ex}} = 488$ nm, $\lambda_{\text{em}} = 490$ –560 nm), Mito-Tracker Green (0.5 μM , $\lambda_{\text{ex}} = 488$ nm, $\lambda_{\text{em}} = 490$ –560 nm), Lyso-Tracker Green (0.5 μM , $\lambda_{\text{ex}} = 488$ nm, $\lambda_{\text{em}} = 490$ –560 nm) were used.

12. Detection of ectogenic and endogenous H_2O_2 and viscosity in cells

RAW 264.7 cells were treated in different ways. The control group: cells without any treatment. The H_2O_2 group: cells were treated with 300 μM H_2O_2 for 10 min. The LPS group: cells were stimulated by LPS (1 mg/mL, 6 h). The LPS+NAC group: cells were stimulated by LPS and then treated by NAC (1 mM, 1 h). The nystatin group: cells were pre-incubated with 10 μM nystatin for 6 h.

After the above treatments, the cells incubated with **HV-AS** (20 μM) for 30 minutes and then were imaged by using SP8 laser confocal microscope. The excitation wavelength of H_2O_2 imaging was set to 561 nm, and the light collection window range was 570–720 nm. The excitation wavelength for viscosity imaging was set at 405 nm, and the light collection window range was 420–550 nm.

13. Fluorescence imaging of HV-AS in cells

The adherent RAW 264.7 cells were treated with different substances. The control group: cells without any treatment. The ox-LDL group: cells were stimulated with 20 $\mu\text{g}/\text{mL}$ ox-LDL for 24 h. The apocynin + ox-LDL group: cells were treated with 100 μM apocynin for 1h, and then were incubated with 20 $\mu\text{g}/\text{mL}$ ox-LDL for 24 h. The setanaxib + ox-LDL group: cells were treated with 10 μM setanaxib for 1.5 h, and then were treated with 20 $\mu\text{g}/\text{mL}$ ox-LDL for 24 h. All of the cells were incubated with **HV-AS** (20 μM) for 30 minutes and then were imaged by using SP8 laser confocal microscope.

The RAW 264.7 cells were stimulated with 20 $\mu\text{g}/\text{mL}$ ox-LDL at various intervals (0, 8, 16, 24 h). Then, cells were incubated with the **HV-AS** (20 μM) for 30 min to observe changes in fluorescence intensity. H_2O_2 channel: $\lambda_{\text{ex}} = 561$ nm, $\lambda_{\text{em}} = 570$ –720 nm; viscosity channel: $\lambda_{\text{ex}} = 405$ nm, $\lambda_{\text{em}} = 420$ –550 nm.

14. Immunofluorescence staining

Cells were divided into the control group, ox-LDL group, apocynin + ox-LDL group and setanaxib + ox-LDL group, which were pretreated as mentioned before. After that, the cells were fixed with 4% paraformaldehyde for 15min at room temperature and subsequently incubated with 0.1% TritonX-100 in PBS for 20 min. Next, the cells were blocked with 5% BSA solution for 1h at 37°C before incubated with primary antibody. Then, the cells were incubated with different primary antibodies (Recombinant Anti-cd40 Rabbit Monoclonal Antibody (1:200), IL-1 β Rabbit Polyclonal Antibody (1:200), LOX-1 Rabbit Polyclonal Antibody (1:200) separately overnight at 4°C. The cells were washed by PBS three times and incubated with Goat Anti-Rabbit IgG H&L (1:1000) for 30 min at 37°C. Nuclei were stained with Hoechst 33342 (1:1000, Beyotime). Fluorescence was detected by SP8 laser confocal microscope. Goat Anti-Rabbit IgG H&L channel: $\lambda_{\text{ex}} = 561$ nm, $\lambda_{\text{em}} = 570$ –720 nm; Hoechst 33342 channel: $\lambda_{\text{ex}} = 405$ nm, $\lambda_{\text{em}} = 420$ –550 nm.

15. In vivo toxicity of HV-AS

The C57BL/6J mice were divided into two groups consisting of control group mice and **HV-AS** group mice. The control group mice: Male C57BL/6J mice at 4 weeks of age were administered tail vein injection with saline (200 μL , per 25g mice) every day for a week. The HV-AS group mice: Male C57BL/6J mice at 4 weeks of age were accepted tail vein injection with **HV-AS** (200 μL , 100 $\mu\text{M}/25\text{g}$ mice) every day for a week. The body weights of two groups of mice were recorded every day for a week. After injection with saline or **HV-AS**, hematoxylin and eosin (H&E) staining of major organ tissues (liver, spleen, lung, heart, and kidney) were conducted to identify the histological changes. The tissues samples were fixed with 4% paraformaldehyde, and dehydrated, embedded, sectioned and stained by hematoxylin and eosin. Finally, the sections were imaged using an optical microscope (Nikon, Eclipse Ci-L).

16. Establishment of mice model

All animal experiments were conducted in accordance with the Guidelines for Animal Experiments of Shandong Normal University. The assigned approval number of the Shandong Normal University was AEECDNU2024016.

Mice were fed and handled in different ways. The control group mice: Male C57BL/6J mice at 4 weeks of age were fed with normal diet for 18 weeks. At 12 week, these mice were injected with saline (1 mg/kg/day) for 6 weeks. The ApoE^{-/-}/HF group mice: Male ApoE^{-/-} mice at 4 weeks of age were fed with a high fat diet for 18 weeks. At 12 week, they were injected with saline (1 mg/kg/day) for

SUPPORTING INFORMATION

6 weeks. The ApoE^{-/-}/HF/setanaxib group mice: Male ApoE^{-/-} mice were at 4 weeks of age were fed with a high fat diet for 18 weeks. At 12 week, they were treated by i.p. injections with setanaxib (1 mg/kg/day). After the mice were fed and treated, they were injected with HV-AS and then imaged.

17. Fluorescence imaging of HV-AS in mice

The control group mice, ApoE^{-/-}/HF group mice and ApoE^{-/-}/HF/setanaxib group mice were administered tail vein injection with HV-AS (100 μ L, 100 μ M/25g mice). After 30 min, fluorescence imaging of the aorta of mice were acquired by using IVIS[®] Lumina III *in vivo* imaging system. H₂O₂ channel: λ_{ex} =580 nm, λ_{em} =670 nm.

And the fluorescence of HV-AS in frozen sections of the aorta were detected though Leica SP8 high-resolution fluorescence microscope. H₂O₂ channel: λ_{ex} =561 nm, λ_{em} =570–720 nm; viscosity channel: λ_{ex} =405 nm, λ_{em} =420–550 nm.

18. Hemolysis test

For hemocompatibility assay, 1 mL of 2% fresh mouse red blood cell (RBC) PBS solution was incubated with water, different concentrations (0, 10, 50, 100, 200 μ M) of HV-AS and 0.1% Triton X-100 at 37°C for 1h, respectively. After centrifugation, hemoglobin content in the supernatant was determined in triplicate by measuring the absorption at 540 nm. The water and 0.1% Triton X-100 were the negative and positive control groups, respectively. The hemolysis rate was calculated as:

$$\text{Hemolysis (\%)} = \frac{A_{\text{sample}} - A_{\text{negative}}}{A_{\text{positive}} - A_{\text{negative}}}$$

Results and Discussion

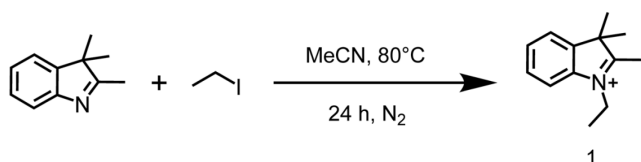


Figure S1. Synthesis route of compound 1.

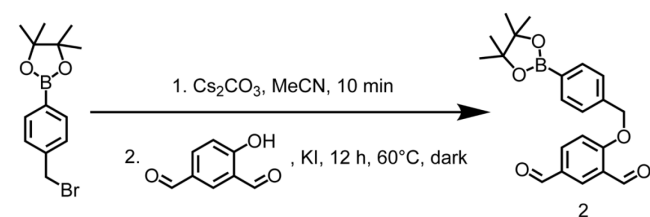


Figure S2. Synthesis route of compound 2.

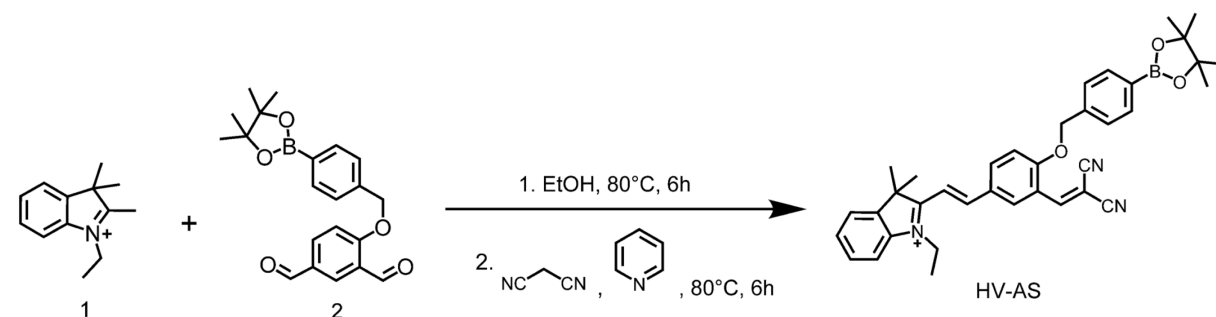


Figure S3. Synthesis route of HV-AS.

SUPPORTING INFORMATION

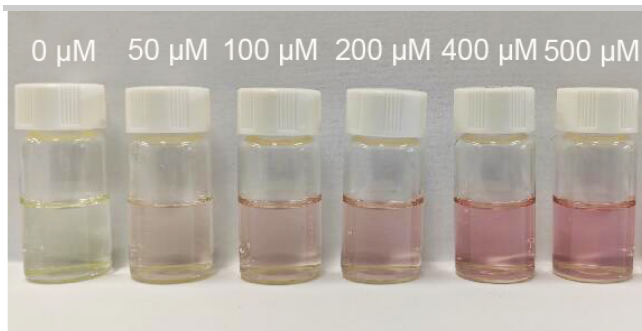


Figure S4. Color changes of HV-AS (20 μM) with different concentrations of H_2O_2 .

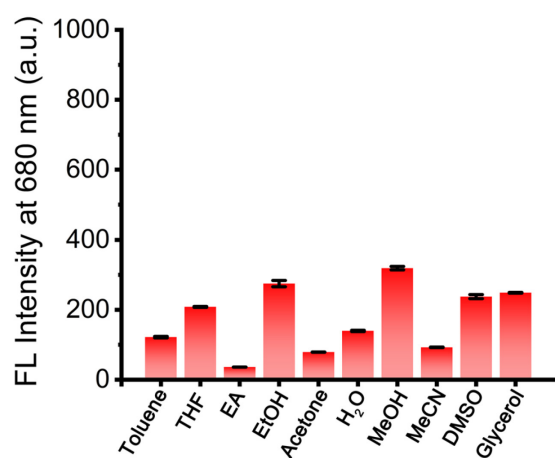


Figure S5. Fluorescence behavior of HV-AS (20 μM) in different polar solvents. $\lambda_{\text{ex/em}} = 570/680 \text{ nm}$.

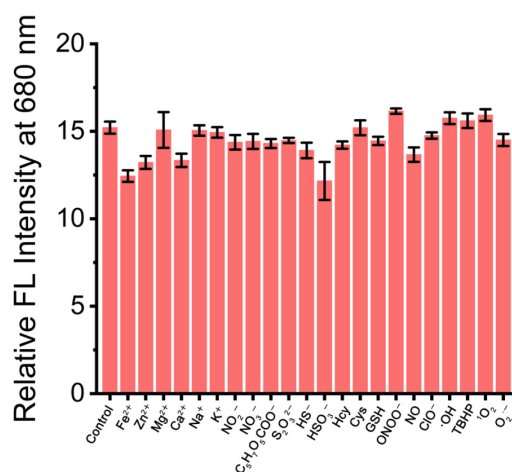


Figure S6. The anti-interference ability for H_2O_2 detection. $\lambda_{\text{ex/em}} = 570/680 \text{ nm}$.

SUPPORTING INFORMATION

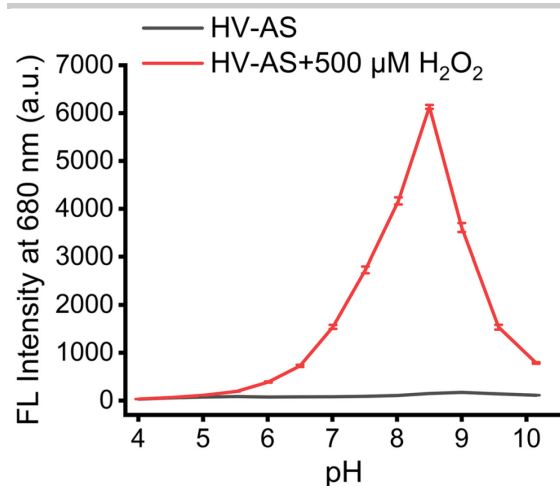


Figure S7. Fluorescence intensity of **HV-AS** (20 μM) in PBS (30% MeCN) after adding 0 μM and 500 μM H_2O_2 with different pHs. $\lambda_{\text{ex/em}}$ = 570/680 nm.

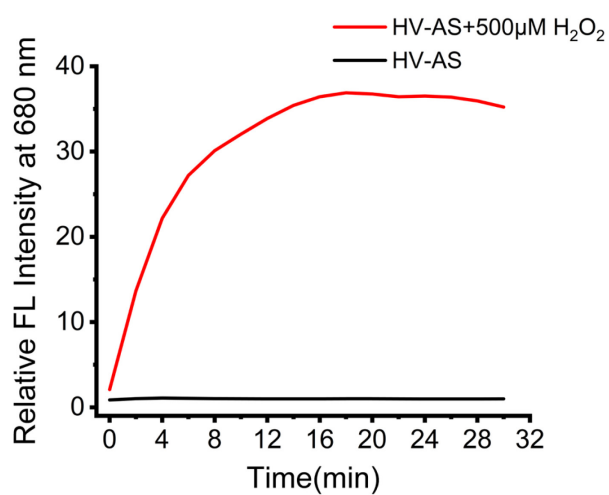


Figure S8. Kinetic parameters of **HV-AS** (20 μM) after adding 0 μM and 500 μM H_2O_2 . $\lambda_{\text{ex/em}}$ = 570/680 nm.

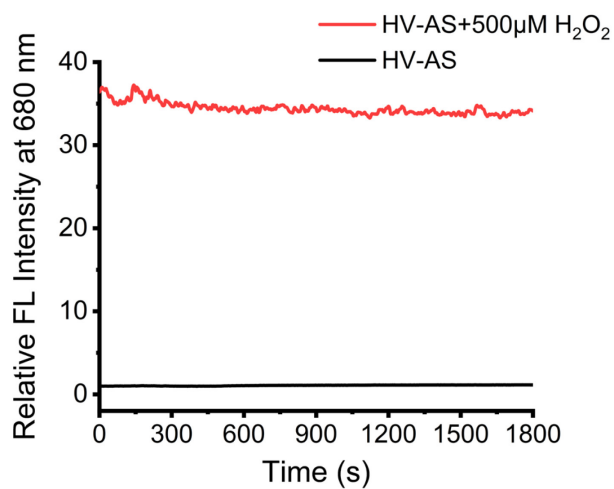


Figure S9. Photostability of **HV-AS** (20 μM) after adding 0 μM and 500 μM H_2O_2 and incubating for 20 min. $\lambda_{\text{ex/em}}$ = 570/680 nm.

SUPPORTING INFORMATION

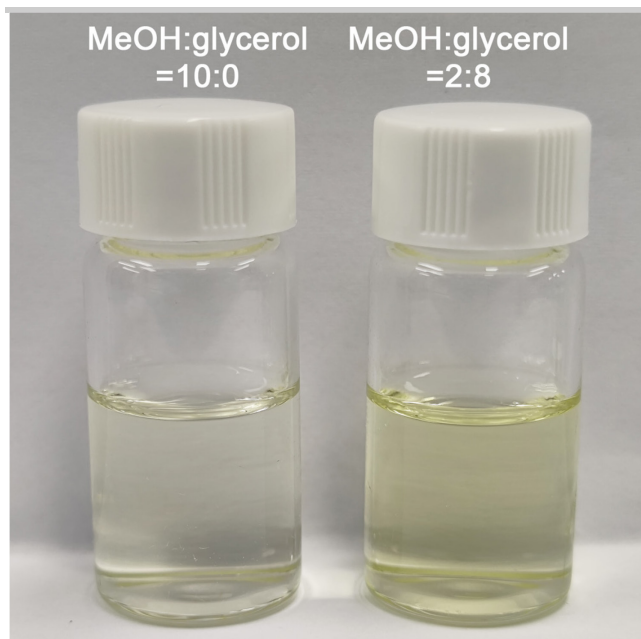


Figure S10. Color changes of HV-AS (20 μM) in different viscosity solutions. $\lambda_{\text{ex/em}} = 360/537 \text{ nm}$.

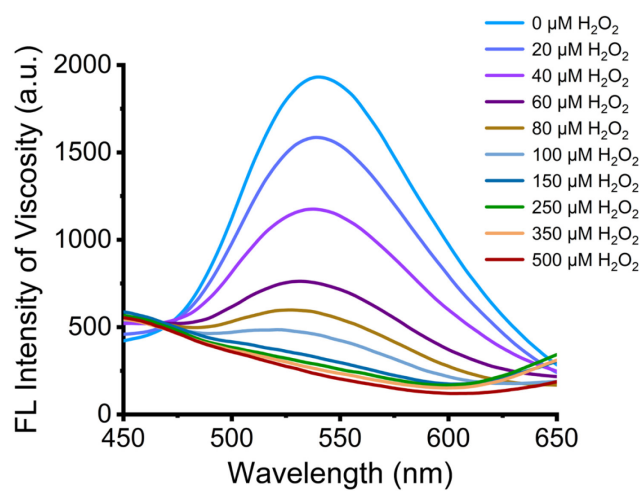
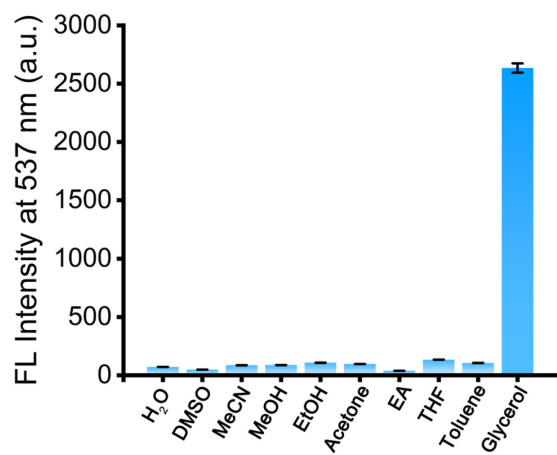


Figure S11. Fluorescence intensity of HV-AS (20 μM) in MeOH-glycerol (2:8, v/v) system after adding 0 μM to 500 $\mu\text{M H}_2\text{O}_2$. $\lambda_{\text{ex}} = 360 \text{ nm}$, $\lambda_{\text{em}} = 450\text{--}650 \text{ nm}$.



SUPPORTING INFORMATION

Figure S12. Fluorescence behavior of **HV-AS** (20 μ M) in different polar solvents. $\lambda_{ex/em}$ = 360/537 nm.

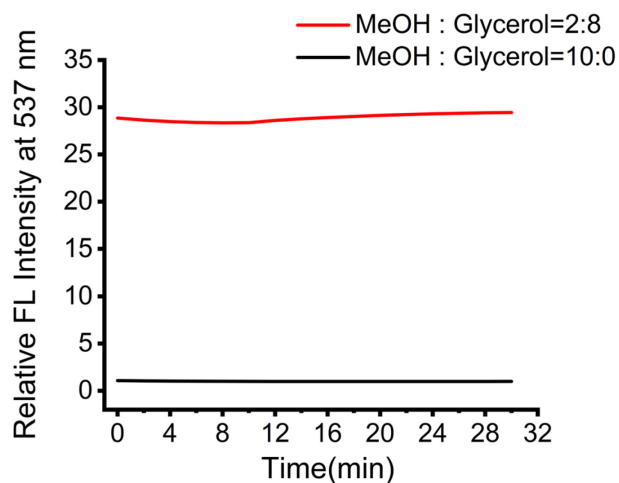


Figure S13. Kinetic parameters of **HV-AS** (20 μ M) in MeOH-glycerol (10:0, v/v) and MeOH-glycerol (2:8, v/v). $\lambda_{ex/em}$ = 360/537 nm.

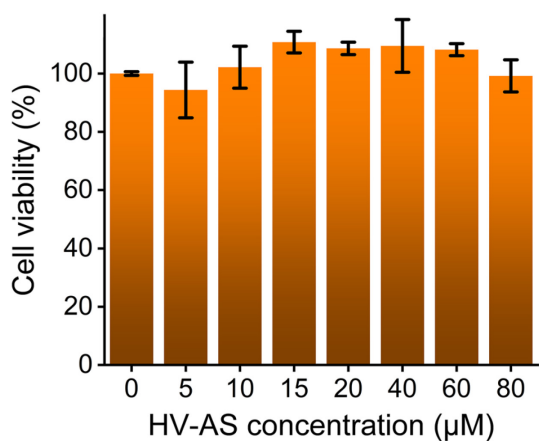


Figure S14. Cell viabilities (%) were estimated by an MTT assay (RAW 264.7 cells). Data are shown as mean \pm SD (n = 3).

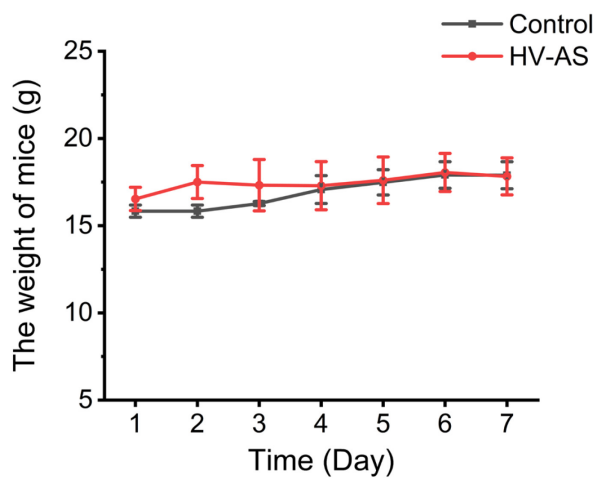


Figure S15. The weight of mice by administering tail vein injection with saline or **HV-AS** for 7 days. The data are expressed as the mean \pm SD (n=3).

SUPPORTING INFORMATION

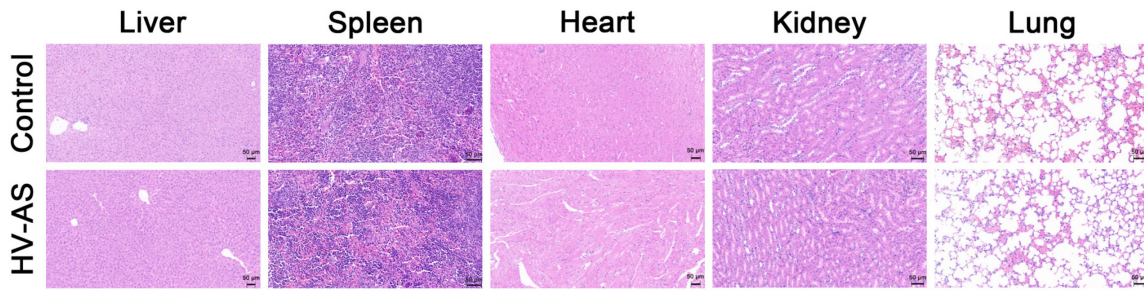


Figure S16. H&E staining of liver, spleen, heart, kidney and lung in control and HV-AS mice. The data are expressed as the mean±SD (n=3).

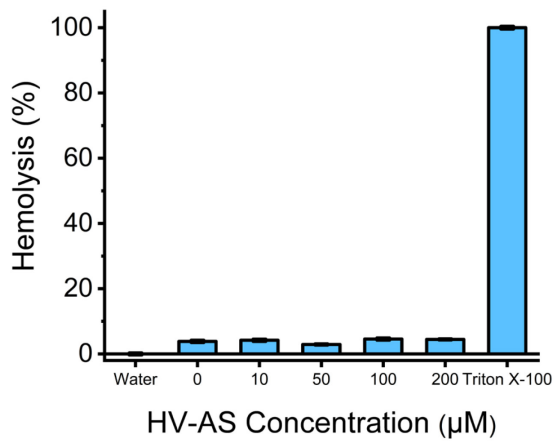
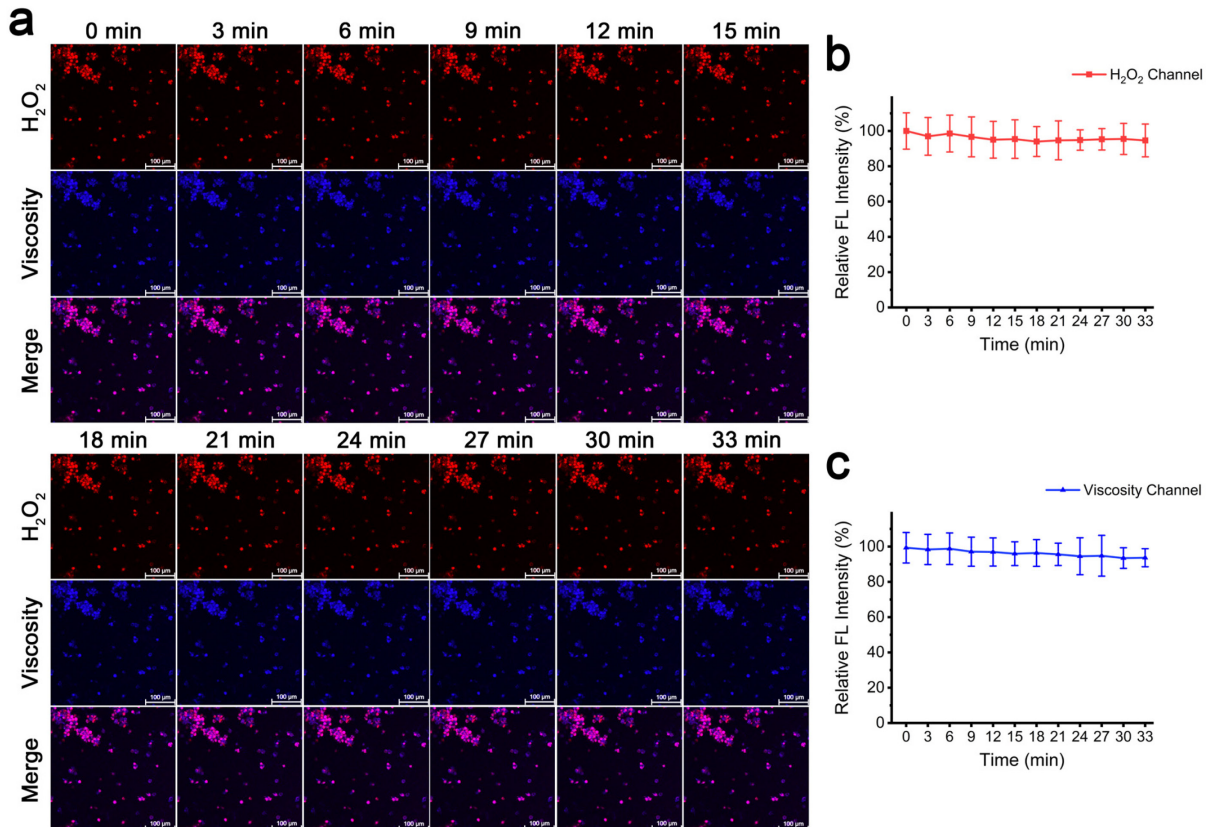


Figure S17. Hemolysis(%) of HV-AS in mice. The data are expressed as the mean±SD (n=3).



SUPPORTING INFORMATION

Figure S18. Photostability of **HV-AS** (20 μ M) in RAW 264.7 cells. (a) Fluorescence imaging of changes in H_2O_2 and viscosity levels within 33 min. (b,c) Data output diagram of (a). H_2O_2 channel: λ_{ex} = 561 nm, λ_{em} = 570–720 nm; viscosity channel: λ_{ex} = 405 nm, λ_{em} = 420–550 nm. The fluorescence intensity of control group was defined as 100%. Data are shown as mean \pm SD (n = 3).

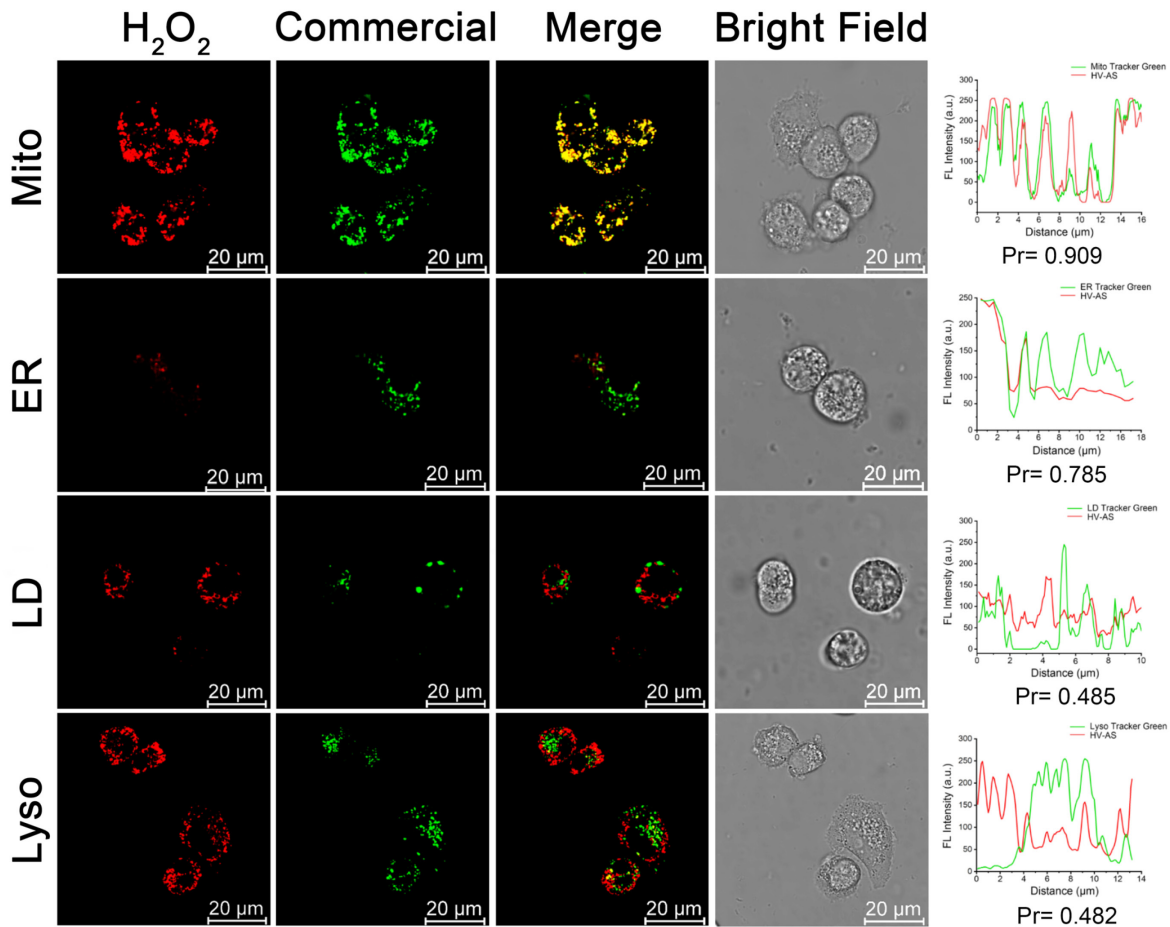


Figure S19. Co-localization fluorescence imaging of **HV-AS** (H_2O_2 channel) and commercial dyes in Hepa 1-6 cells. H_2O_2 channel: λ_{ex} = 561 nm, λ_{em} = 570–720 nm; LD-Tracker Green: λ_{ex} = 488 nm, λ_{em} = 490–560 nm; ER-Tracker Green: λ_{ex} = 488 nm, λ_{em} = 490–560 nm; Mito-Tracker Green: λ_{ex} = 488 nm, λ_{em} = 490–560 nm; Lyso-Tracker Green: λ_{ex} = 488 nm, λ_{em} = 490–560 nm. Data are shown as mean \pm SD (n = 3).

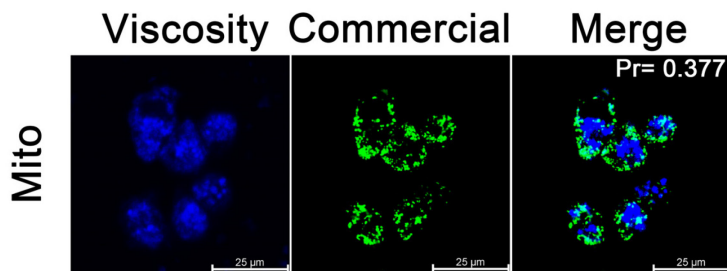


Figure S20. Co-localization fluorescence imaging of **HV-AS** (viscosity channel) and commercial dyes in Hepa 1-6 cells. Viscosity channel: λ_{ex} = 405 nm, λ_{em} = 420–550 nm; Mito-Tracker Green: λ_{ex} = 488 nm, λ_{em} = 490–560 nm. Data are shown as mean \pm SD (n = 3).

SUPPORTING INFORMATION

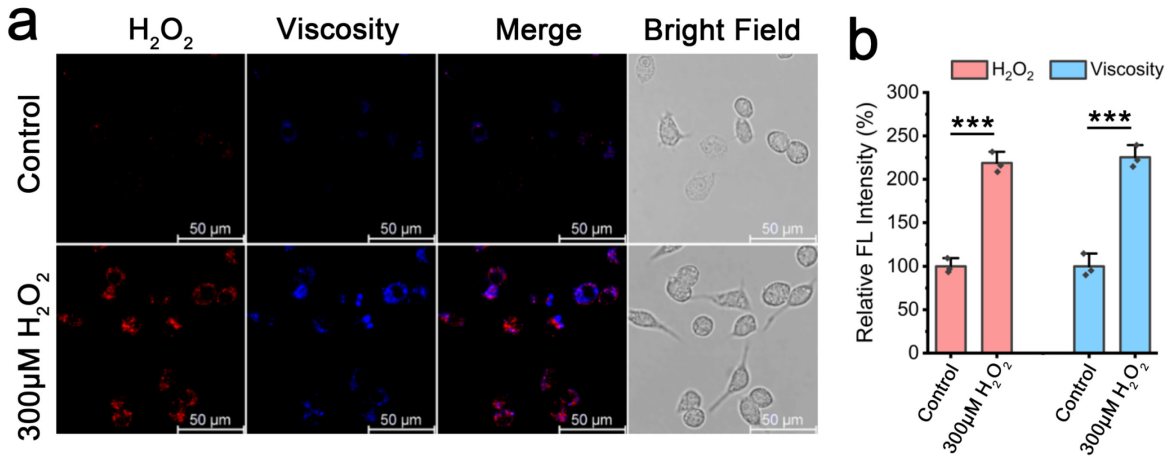


Figure S21. (a) Response of **HV-AS** to exogenous H₂O₂ in RAW 264.7 cells. (b) Data output diagram of (a). H₂O₂ channel: λ_{ex} = 561 nm, λ_{em} = 570–720 nm; viscosity channel: λ_{ex} = 405 nm, λ_{em} = 420–550 nm. The fluorescence intensity of control group was defined as 100%. Data are shown as mean \pm SD (n = 3). ***p < 0.001.

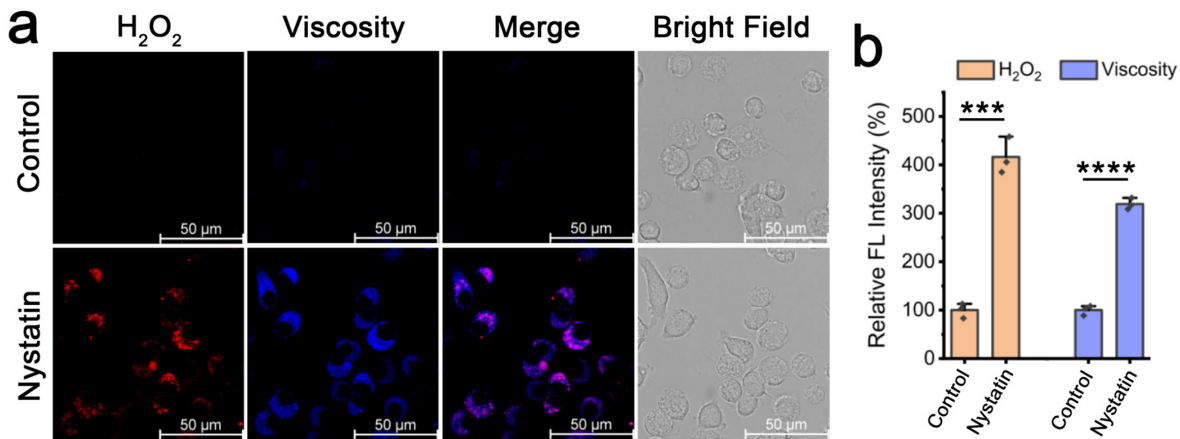
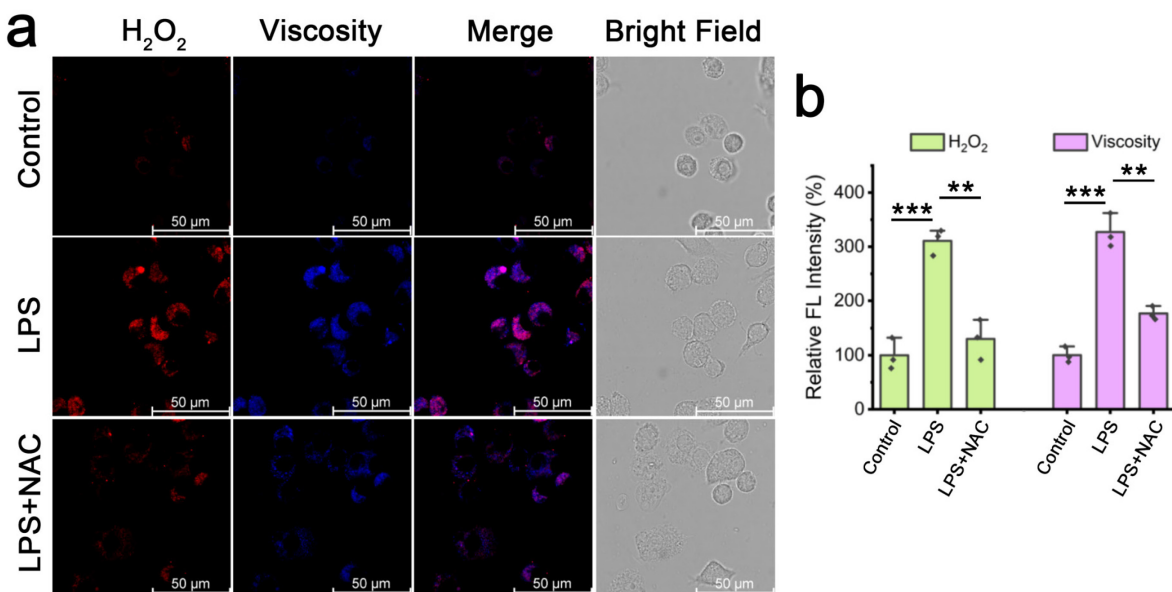


Figure S22. (a) Response of **HV-AS** to endogenous viscosity in RAW 264.7 cells. (b) Data output diagram of (a). H₂O₂ channel: λ_{ex} = 561 nm, λ_{em} = 570–720 nm; viscosity channel: λ_{ex} = 405 nm, λ_{em} = 420–550 nm. The fluorescence intensity of control group was defined as 100%. Data are shown as mean \pm SD (n = 3). ****p < 0.0001, ***p < 0.001.



SUPPORTING INFORMATION

Figure S23. (a) Response of HV-AS to endogenous H_2O_2 in RAW 264.7 cells. (b) Data output diagram of (a). H_2O_2 channel: $\lambda_{ex} = 561$ nm, $\lambda_{em} = 570-720$ nm; viscosity channel: $\lambda_{ex} = 405$ nm, $\lambda_{em} = 420-550$ nm. The fluorescence intensity of control group was defined as 100%. Data are shown as mean \pm SD (n = 3). ***p < 0.001, **p < 0.01.

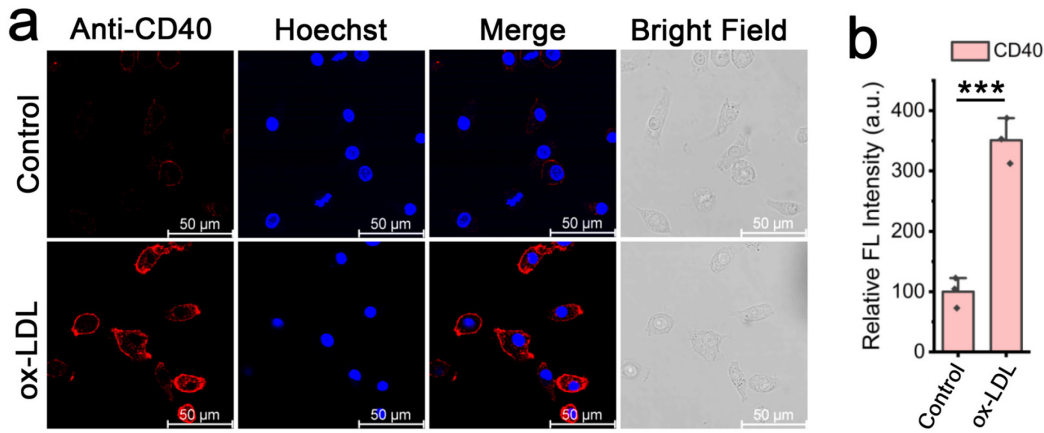


Figure S24. (a) Immunofluorescence images of CD40 and Hoechst 33342 indicated CD40 epitopes (red fluorescence) and nucleus (blue fluorescence). (b) Data output diagram of (a). Red fluorescence channel: $\lambda_{ex} = 561$ nm, $\lambda_{em} = 570-720$ nm; blue fluorescence channel: $\lambda_{ex} = 405$ nm, $\lambda_{em} = 420-550$ nm. The fluorescence intensity of control group was defined as 100%. The data are expressed as the mean \pm SD (n=3). ***p < 0.001.

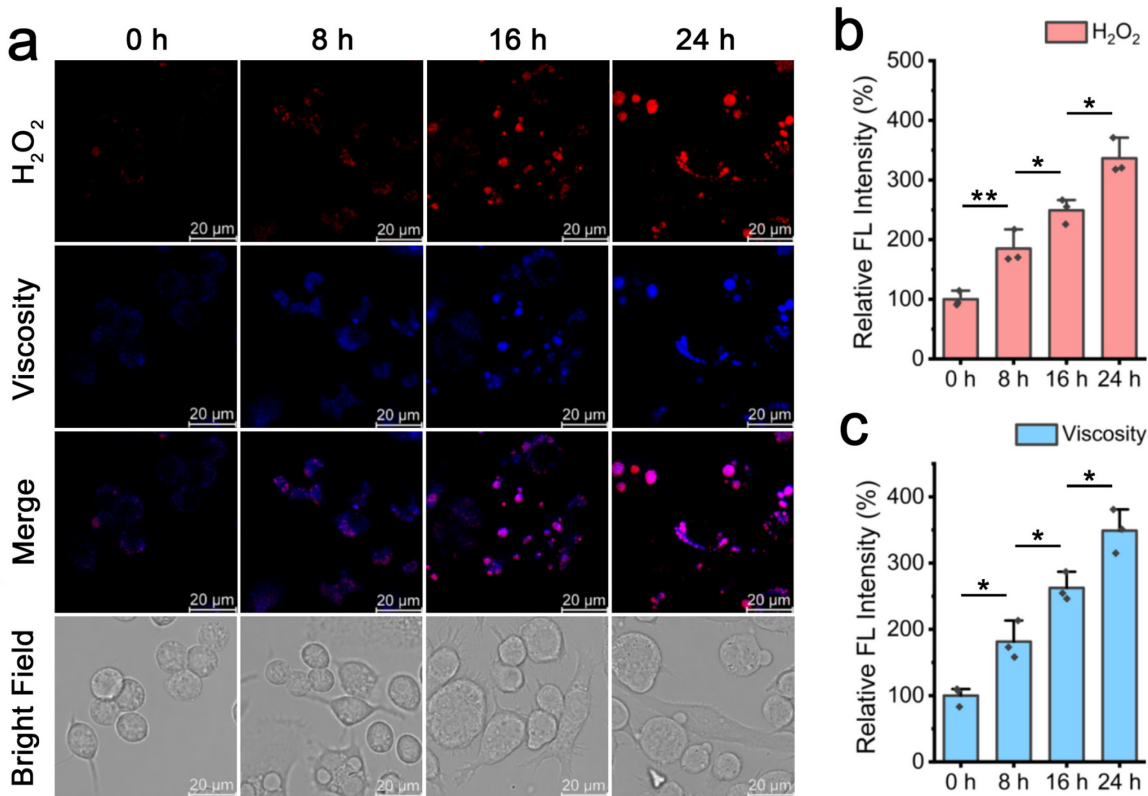


Figure S25. (a) Fluorescence imaging of changes in H_2O_2 and viscosity levels during foam cell formation by HV-AS. (b,c) Data output diagram of (a). The fluorescence intensity of control group was defined as 100%. H_2O_2 channel: $\lambda_{ex} = 561$ nm, $\lambda_{em} = 570-720$ nm; viscosity channel: $\lambda_{ex} = 405$ nm, $\lambda_{em} = 420-550$ nm. Data are shown as mean \pm SD (n = 3). **p < 0.01, *p < 0.05.

SUPPORTING INFORMATION

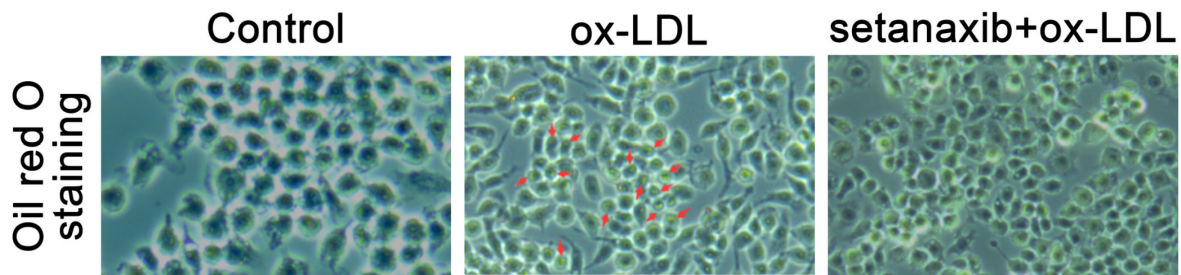


Figure S26. Oil red O staining of RAW 264.7 cells. The data are expressed as the mean \pm SD (n=3).

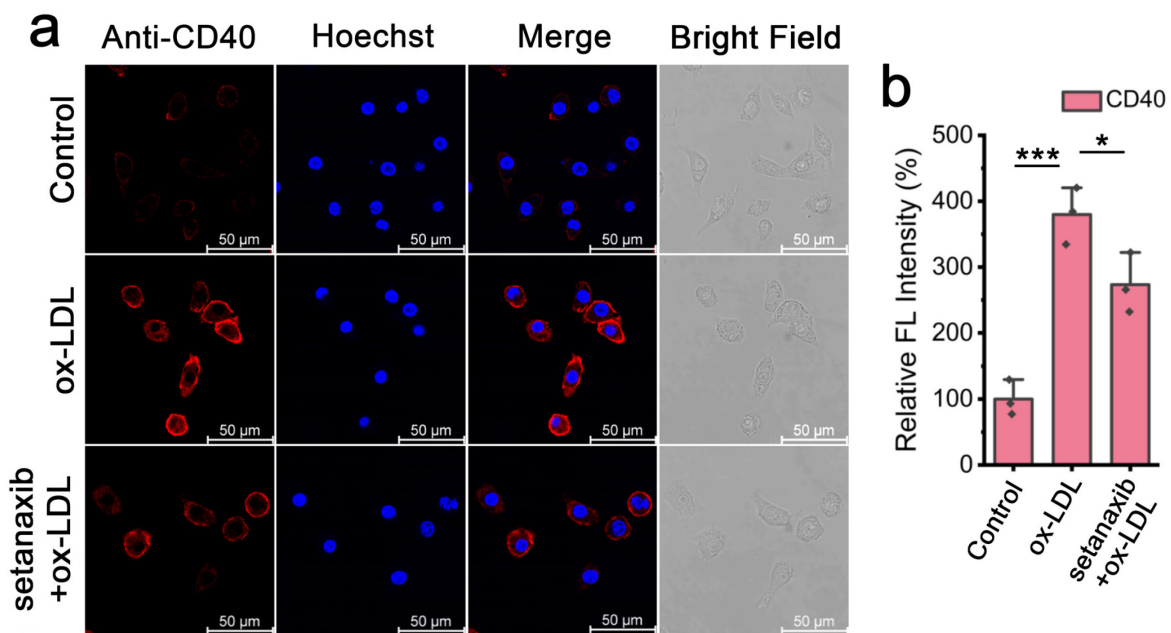


Figure S27. (a) Immunofluorescence images of CD40 and Hoechst 33342 indicated CD40 epitopes (red fluorescence) and nucleus (blue fluorescence). (b) Data output diagram of (a). Red fluorescence channel: $\lambda_{\text{ex}} = 561 \text{ nm}$, $\lambda_{\text{em}} = 570\text{--}720 \text{ nm}$; blue fluorescence channel: $\lambda_{\text{ex}} = 405 \text{ nm}$, $\lambda_{\text{em}} = 420\text{--}550 \text{ nm}$. The fluorescence intensity of control group was defined as 100%. The data are expressed as the mean \pm SD (n=3). ***p < 0.001, *p < 0.05.

SUPPORTING INFORMATION

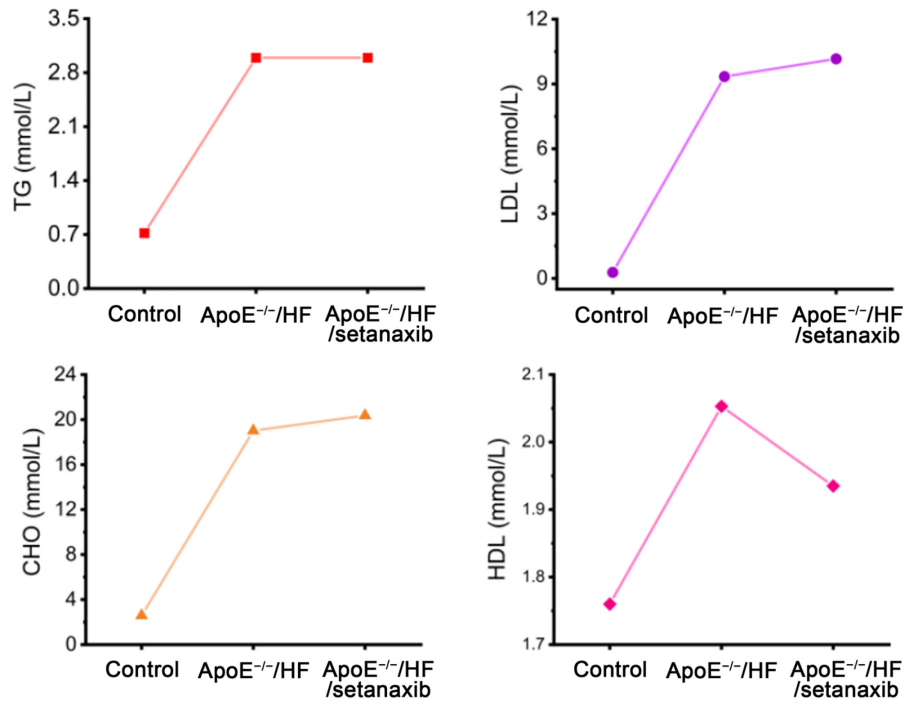


Figure S28. The levels of TG, CHO, LDL and HDL in the serum of mice.

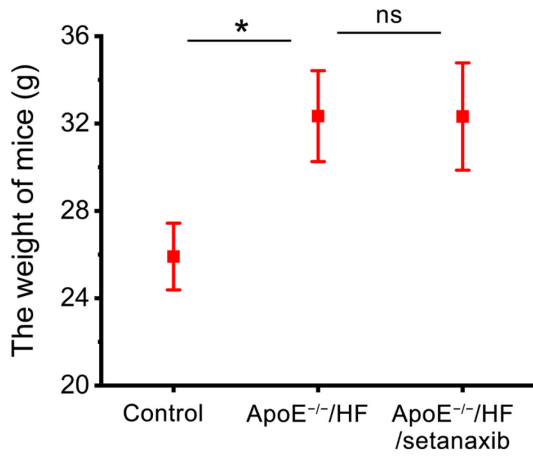


Figure S29. The weight of mice. The data are expressed as the mean \pm SD (n=3). ns: no significance, *p < 0.05.

SUPPORTING INFORMATION

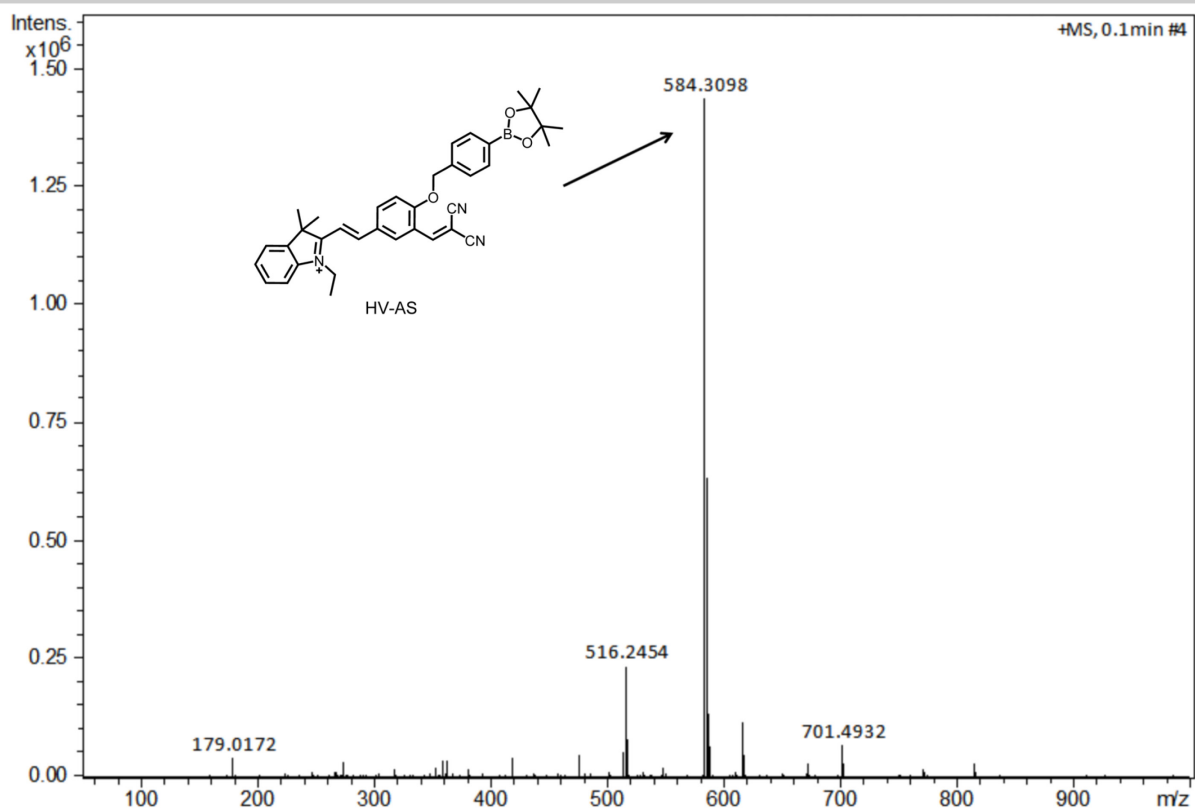


Figure S30. The HRMS(ESI) of HV-AS.

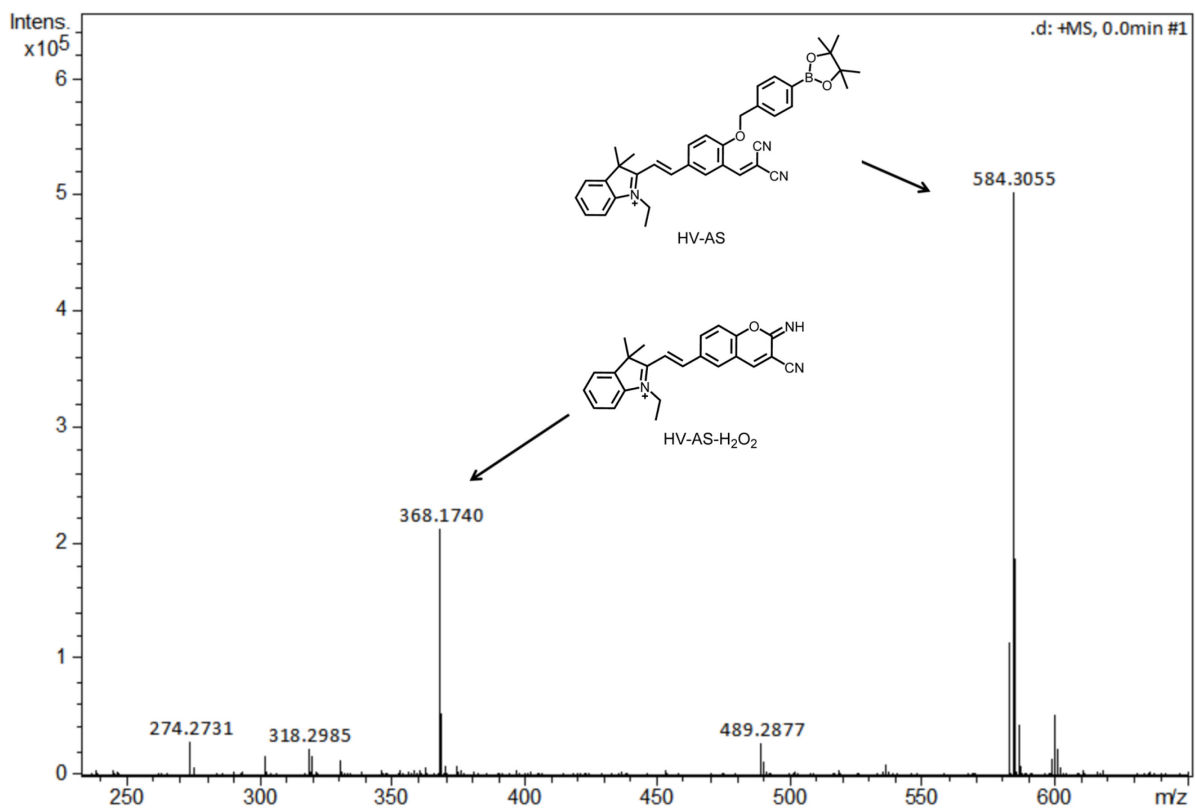


Figure S31. The HRMS(ESI) of HV-AS and HV-AS-H₂O₂.

SUPPORTING INFORMATION

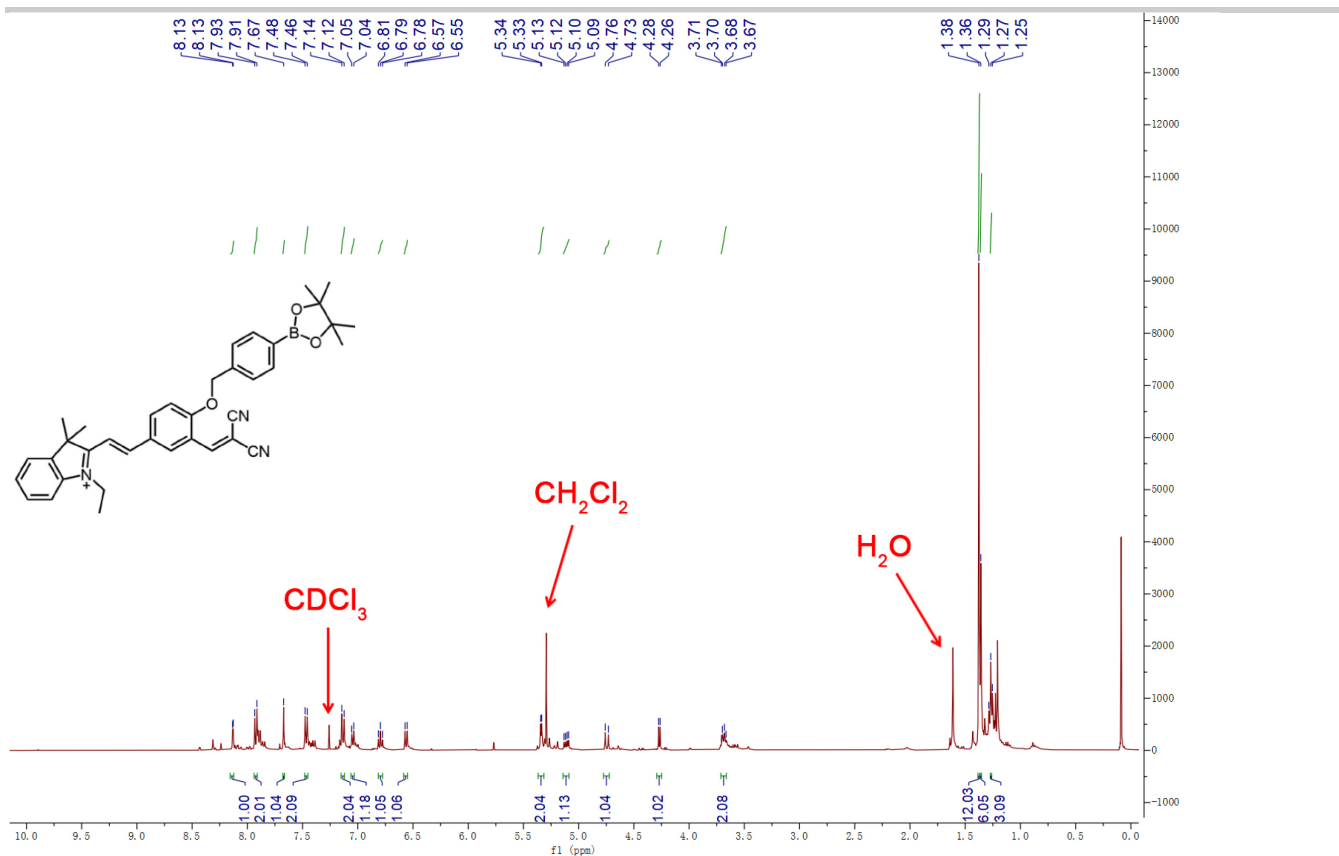


Figure S32. The ¹H NMR of HV-AS.

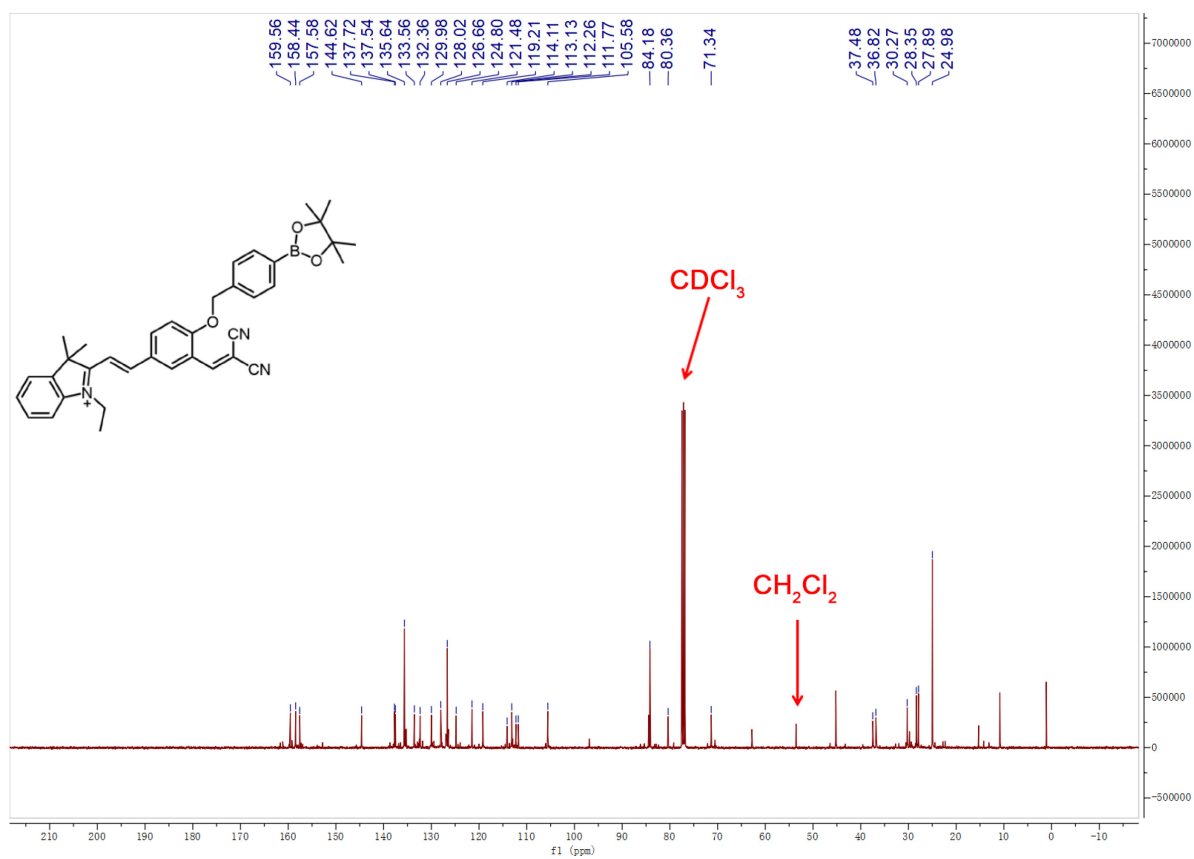
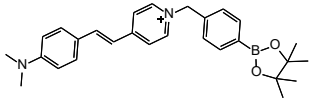
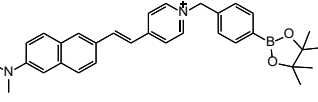
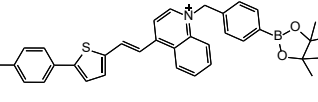
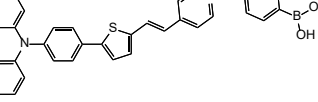
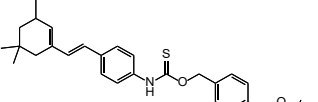
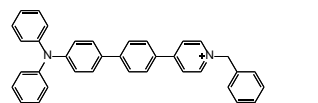
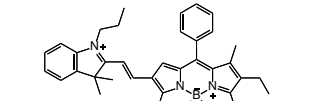
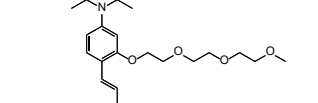


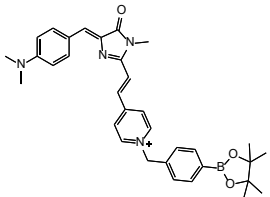
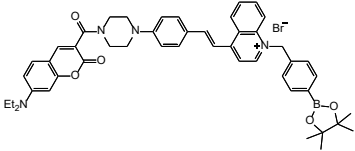
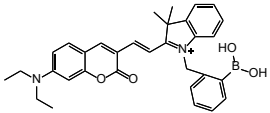
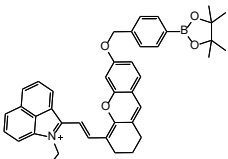
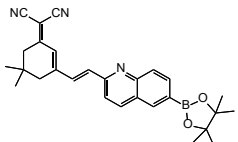
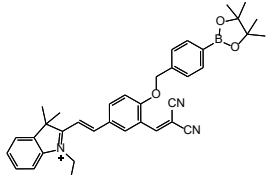
Figure S33. The ¹³C NMR of HV-AS.

SUPPORTING INFORMATION

Table S1: Comparison of Fluorescent Probes for H₂O₂ and viscosity.

Probe ⁵⁻¹⁷	$\lambda_{\text{ex/em}}$, H ₂ O ₂ /nm	LOD (3 σ /k)	Reaction medium (v/v) in H ₂ O ₂ channel	$\lambda_{\text{ex/em}}$, viscosity /nm	Reaction medium (v/v) in viscosity channel	$ \Delta\lambda_{\text{em}} $ /nm	Applications	References
	400 /510	2.1 μM	PBS solution	500 /607	EtOH /Glycerol	97	HeLa cells and RAW 264.7 cells imaging	<i>Anal. Chem.</i> , 2017, 89 , 552–555.
	380 /585	4.98 nM	DMSO /PBS (3/7)	480 /730	MeOH /glycerol	145	HepG2 cells , zebrafish and Drosophila brain imaging in Parkinson's disease (PD)	<i>J. Mater. Chem. B</i> , 2019, 7 , 4243–4251.
	440 /700	3 nM	DMSO /PBS (3/7)	570 /800	EtOH /Glycerol	100	HeLa cells and BALB/c mice imaging in Alzheimer's disease (AD)	<i>Chem. Commun.</i> , 2020, 56 , 1050–1053.
	405 /586	0.141 μM	DMSO /PBS (1/1)	488 /666	MeOH /glycerol	80	HeLa cells imaging, living normal tissue and tumour of KM mice imaging in inflammation and tumor models	<i>Chin. J. Chem.</i> , 2021, 39 , 1303–1309.
	469 /667	0.37 μM	DMSO /PBS (1/9)	469 /815	PBS /Glycerol	148	H9C2 cells imaging in inflammation therapy	<i>Talanta</i> , 2021, 235 , 122719.
	405 /460	4.2 μM	DMSO /PBS (1/9)	405 /614	EtOH /Glycerol	154	HeLa cells, HL-7702 cells, 3T3 cells and liver tissue imaging in fatty liver tissue	<i>New J. Chem.</i> , 2021, 45 , 12138– 12144.
	720 /835	1.37 μM	DMSO /PBS (4/6)	500 /600	Water /Glycerol	235	HepG2 cells and mice imaging in pyroptosis	<i>Chem. Commun.</i> , 2023, 59 , 12775– 12778.
	440 /570	13 nM	DMSO /PBS (4/6)	570 /670	PBS /Glycerol	100	SH-SY5Y cells and SD rats imaging in cerebral ischemia– reperfusion injury (CIRI)	<i>Anal. Chem.</i> , 2024, 96 , 3436–3444.

SUPPORTING INFORMATION

	-- /660	2.0 μM	PBS solution	-- /635	H ₂ O /Glycerol	25	SH-SY5Y cells, APP/PS1 transgenic mouse imaging in Alzheimer's disease (AD)	<i>Dyes Pigm.</i> , 2022, 206 , 110665.
	450 /550, 671	0.87 μM	THF /PBS (3/7)	450 /660	-- /Glycerol	121	HeLa cells imaging	<i>Talanta</i> , 2024, 275 , 126135.
	410 /522, 590 /670	3.3 μM	DMSO /PBS (1/99)	410 /522, 590 /670	MeOH /glycerol	148	HeLa cells imaging	<i>Bioorg. Chem.</i> , 2022, 119 , 105513.
	808 /945	0.14 μM	PBS solution	700 /810	PBS /Glycerol	135	HeLa cells, tumor tissues, tumor-bearing mice imaging in cancer	<i>Adv. Healthcare Mater.</i> , 2023, 12 , 2301230.
	410 /582	15 nM	PBS /Glycerol (3/7)	410 /475	PBS /Glycerol	107	BV-2 cells and C57BL/6J mice in inflammation	<i>Dyes Pigm.</i> , 2022, 207 , 110664.
	570 /680	0.361 μM	MeCN /PBS (3/7)	360 /537	MeOH /Glycerol	143	RAW 264.7 cells, C57BL/6J mice and ApoE ^{-/-} mice imaging in atherosclerosis	This work

-- Not mentioned.

Table S2: The viscosity of the MeOH-glycerol mixture in different proportions at (28.5 ± 0.1) °C.

MeOH-Glycerol system (v/v)	viscosity (cp)
100: 0	0.3
95: 5	0.5
90: 10	0.7
85:15	1.1
80:20	1.6
75: 25	1.9
70: 30	3.1
65: 35	4.13
60: 40	6.6
55: 45	7.63
50:50	8.67
45: 55	13.43
40: 60	18.7
35: 65	26.2
30: 70	36.0
25: 75	57.6
20: 80	140.0

References

- [1] M. Collot, R. Kreder, A. L. Tatarets, L. D. Patsenker, Y. Mely, A. S. Klymchenko, *Chem. Commun.*, 2015, **51**, 17136–17139.
- [2] H. Xu, Y. Wang, Z. Pei, W. Ji, Y. Pei, *Chem. Commun.*, 2019, **55**, 14930–14933.
- [3] J. Liu, W. Zhang, C. Zhou, M. Li, X. Wang, W. Zhang, Z. Liu, L. Wu, T. D. James, P. Li, *J. Am. Chem. Soc.*, 2022, **144**, 13586–13599.
- [4] Z. Wang, S. Wang, B. Wang, J. Shen, L. Zhao, F. Yu, J. T. Hou, *Chem. Eng. J.*, 2023, **464**, 142687–142695.
- [5] M. Ren, B. Deng, K. Zhou, X. Kong, J. Y. Wang, W. Lin, *Anal. Chem.*, 2017, **89**, 552–555.
- [6] H. Li, C. Xin, G. Zhang, X. Han, W. Qin, C. W. Zhang, C. Yu, S. Jing, L. Li, W. Huang, *J. Mater. Chem. B*, 2019, **7**, 4243–4251.
- [7] S. Li, P. Wang, W. Feng, Y. Xiang, K. Dou, Z. Liu, *Chem. Commun.*, 2020, **56**, 1050–1053.
- [8] L. Fan, Q. Zan, X. Wang, S. Wang, Y. Zhang, W. Dong, S. Shuang, C. Dong, *Chin. J. Chem.*, 2021, **39**, 1303–1309.
- [9] T. Liang, D. Zhang, W. Hu, C. Tian, L. Zeng, T. Wu, D. Lei, T. Qiang, X. Yang, X. Sun, *Talanta*, 2021, **235**, 122719.
- [10] H. Xu, J. Zhong, W. Zhuang, J. Jiang, B. Ma, H. He, G. Li, Y. Liao, Y. Wang, *New J. Chem.*, 2021, **45**, 12138–12144.
- [11] Y. Mei, Z. Li, K. Rong, Z. Hai, W. Tang, Q. H. Song, *Chem. Commun.*, 2023, **59**, 12775–12778.
- [12] C. Fang, Q. Deng, K. Zhao, Z. Zhou, X. Zhu, F. Liu, P. Yin, M. Liu, H. Li, Y. Zhang, S. Yao, *Anal. Chem.*, 2024, **96**, 3436–3444.
- [13] Y. Guo, H. Leng, Y. Wang, W. J. Shi, L. Zhang, J. Yan, *Dyes Pigm.*, 2022, **206**, 110665.
- [14] F. T. Liu, S. Wang, Y. P. Wang, P. F. Jiang, J. Y. Miao, B. X. Zhao, Z. M. Lin, *Talanta*, 2024, **275**, 126135.
- [15] D. Liu, G. Chen, G. Fang, *Bioorg. Chem.*, 2022, **119**, 105513.
- [16] W. X. Wang, J. J. Chao, Z. Q. Wang, T. Liu, G. J. Mao, B. Yang, C. Y. Li, *Adv. Healthcare Mater.*, 2023, **12**, 2301230.
- [17] W. Hu, T. Qiang, L. Ren, B. Wang, T. Liang, C. Li, *Dyes Pigm.*, 2022, **207**, 110664.

Author Contributions

Hui Wang and Jingjing Guo contributed equally to this work. Hui Wang designed the probe, analyzed data and prepared the original draft. Jingjing Guo performed experiments, analyzed data and prepared the original draft. Tiancong Xiu performed parts of the experiments. Yue Tang prepared the original draft. Ping Li and Bo Tang revised the manuscript. Wei Zhang and Wen Zhang analyzed data.